Supplement of Atmos. Chem. Phys. Discuss., 15, 24419–24472, 2015
http://www.atmos-chem-phys-discuss.net/15/24419/2015/
doi:10.5194/acpd-15-24419-2015-supplement

Supplement of

Aerosol properties, source identification, and cloud processing in orographic clouds measured by single particle mass spectrometry on a Central European mountain site during HCCT-2010

A. Roth et al.

Correspondence to: J. Schneider (johannes.schneider@mpic.de)

1. Back trajectories for the whole time period

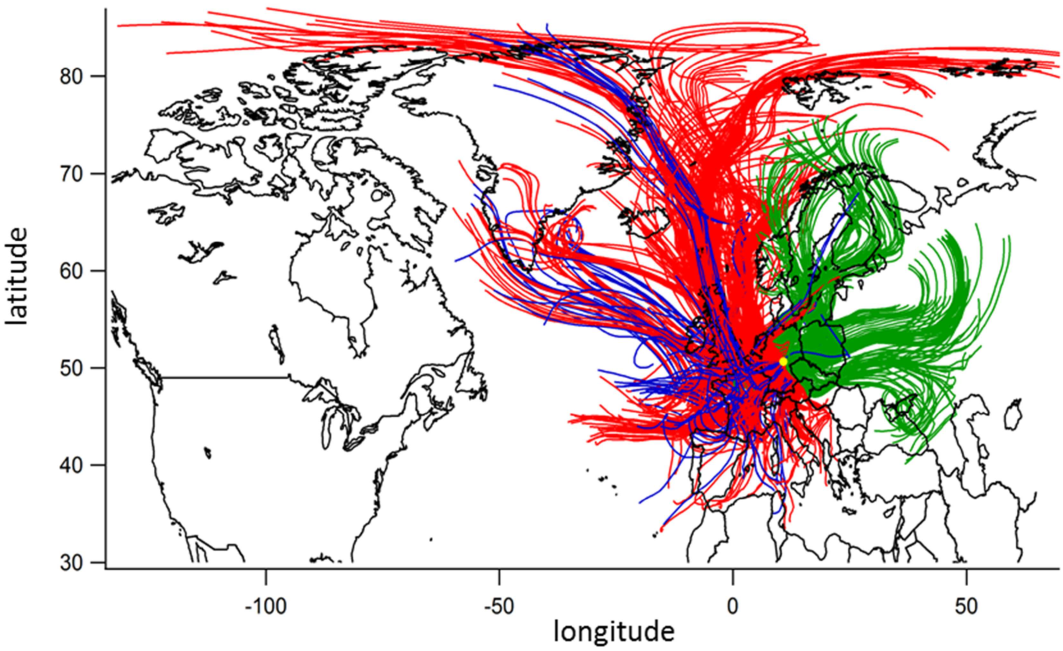

Figure S1: HYSPLIT back trajectories during HCCT-2010 (red). Air masses during FCEs (blue) and with easterly air mass origins (green) are emphasized.

2. Cluster Types

The clustering was initiated with a number of clusters of 200. The algorithm assigned all mass spectra to 159 clusters. These 159 clusters were inspected manually and combined if two mean cluster spectra *j* and *k* showed a Pearson correlation coefficient r_{jk} larger than 0.7. Out of the 65 remaining clusters 19 different fragmentation types plus “others” were determined. These are shown in Figure S2-S5. Each presented cluster spectrum represents a cluster type. In some cases clusters were not combined although they belonged to the same particle type and showed a similar fragmentation pattern. In such cases the Pearson correlation coefficient of the two clusters was smaller than 0.7. For example, cluster type "org, K_1" represents 5 other clusters of the particle type “org, K” showing the same fragmentation but not a sufficient correlation coefficient for combination. The shown representative mean mass spectra of cluster types are averaged over a range of 263 ("Ca") and 11508 ("soot") single particle mass spectra. Table S1 shows the Pearson correlation coefficients for the representative cluster spectra (B1-B4). Correlation coefficients with $r_{jk} \geq 0.7$ are highlighted gray. Especially clusters of the particle types "org, K", "biomass burning", "soot", "soot and org" and "K" look similar and show a larger correlation coefficient than 0.7. Evaluation of the clustering algorithm fuzzy c-means showed that with a smaller number of predetermined start clusters the algorithm combines such mass spectra in one cluster because it cannot be distinguished mathematically between different particle types.

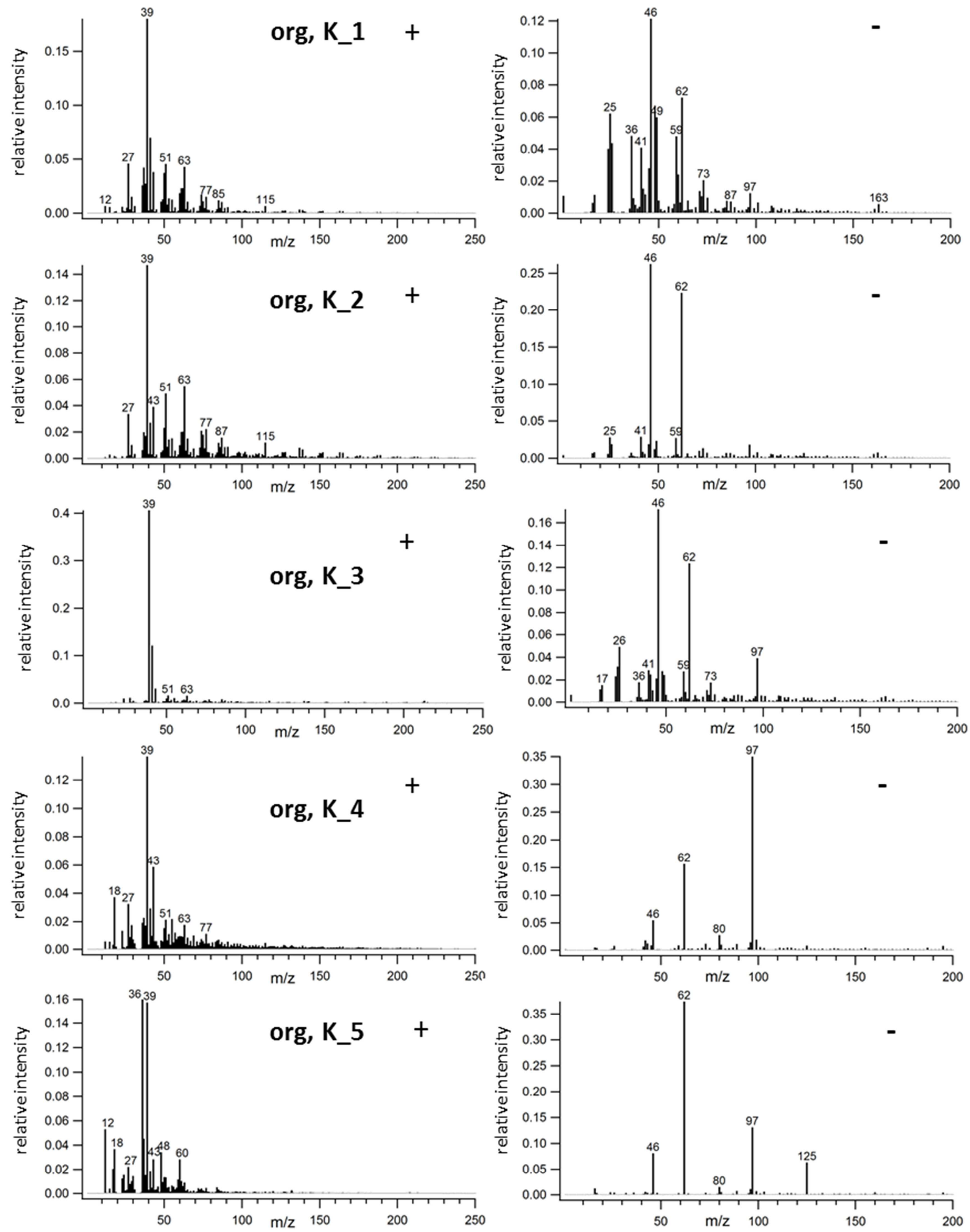

Figure S2: Mean positive (left) and negative (right) mass spectra representative for the different cluster types (25 clusters in total) of the particle type "org, K". The association of ion fragments to specific values for m/z is listed in Table 2.

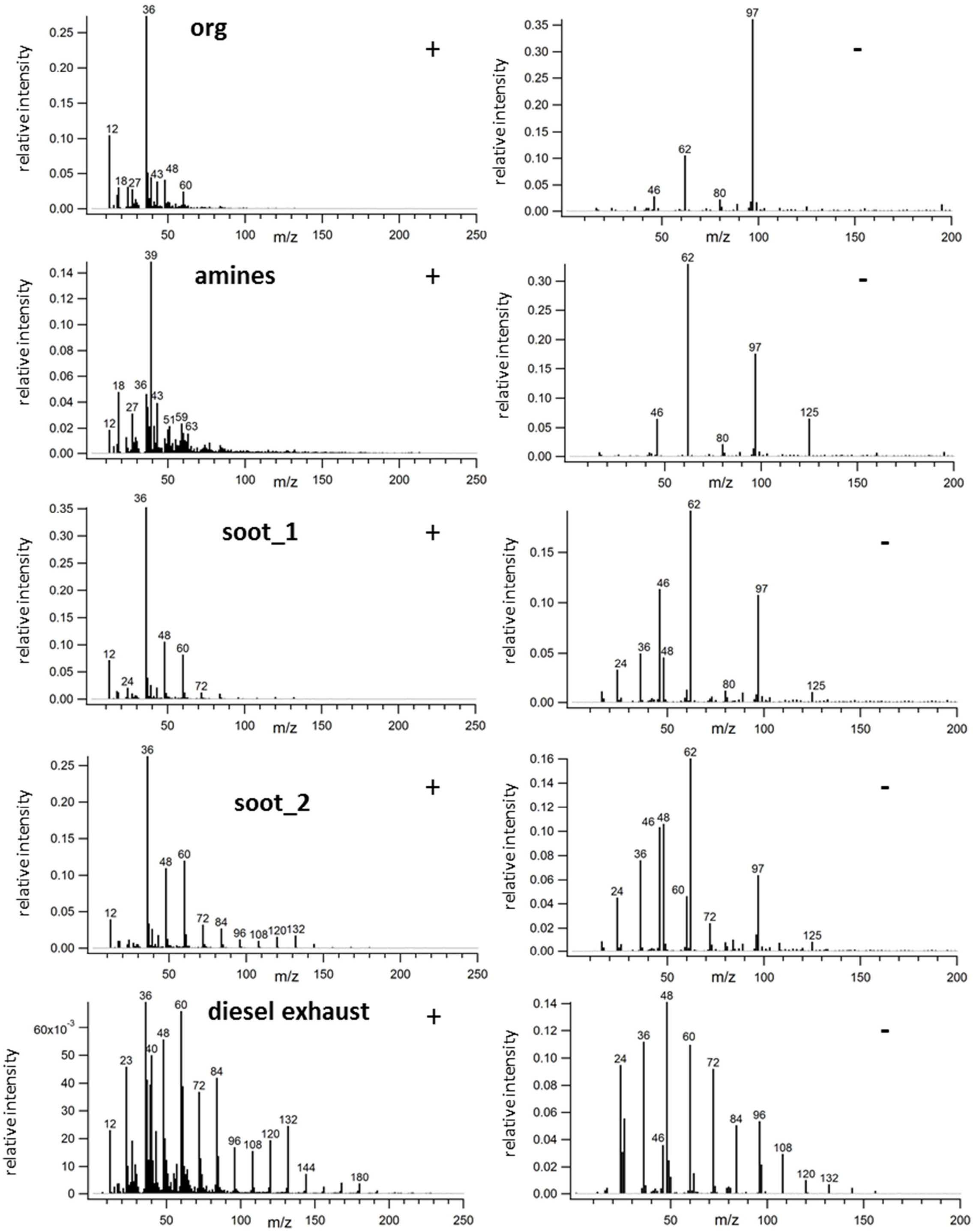

Figure S3: Mean positive (left) and negative (right) mass spectra of the particle types "org" (3 clusters), "amines", "soot" (5 clusters) and "diesel exhaust".

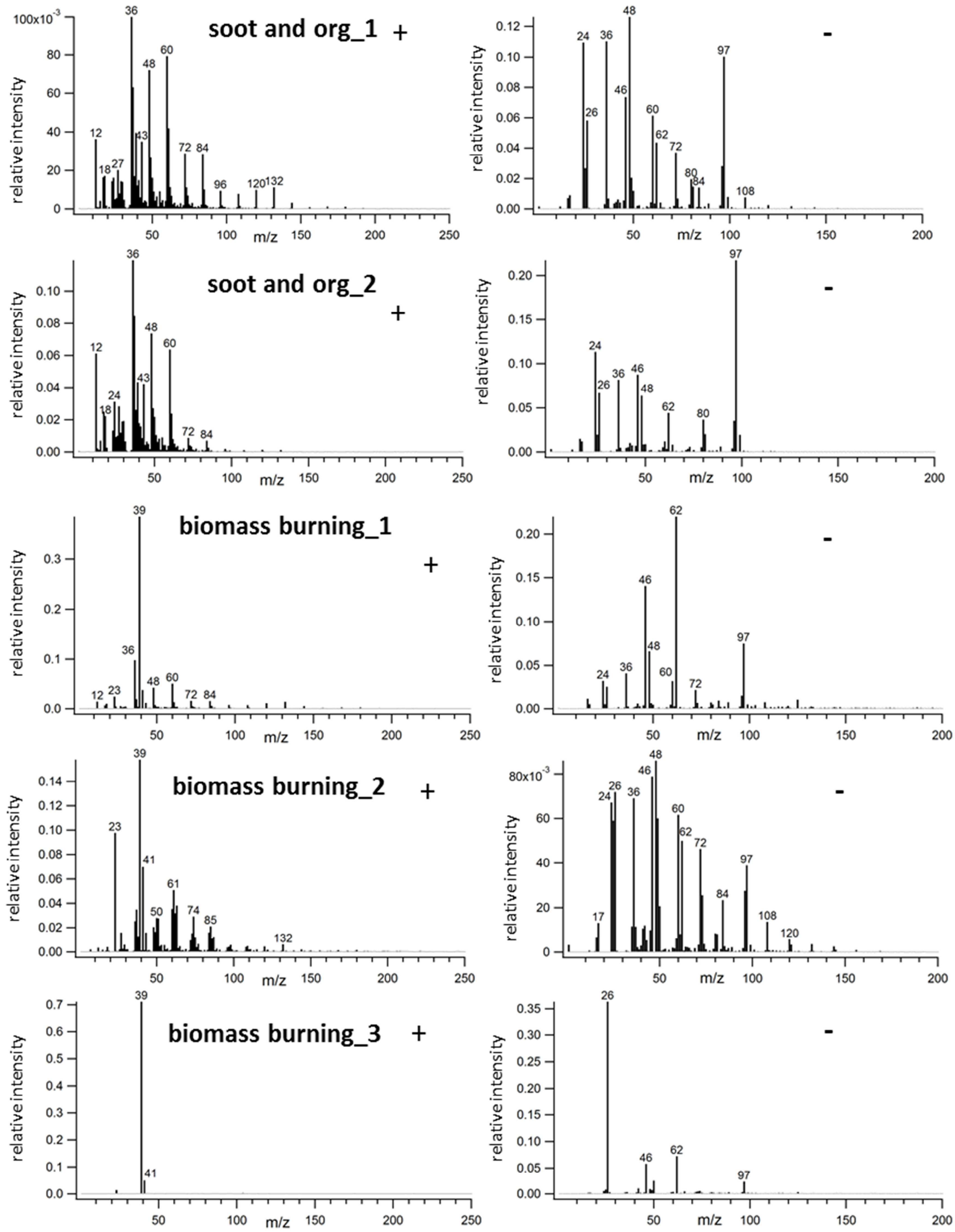

Figure S4: Mean positive (left) and negative (right) mass spectra representative for the different cluster types of the particle types “soot and org” (4 clusters) and “biomass burning” (18 clusters).

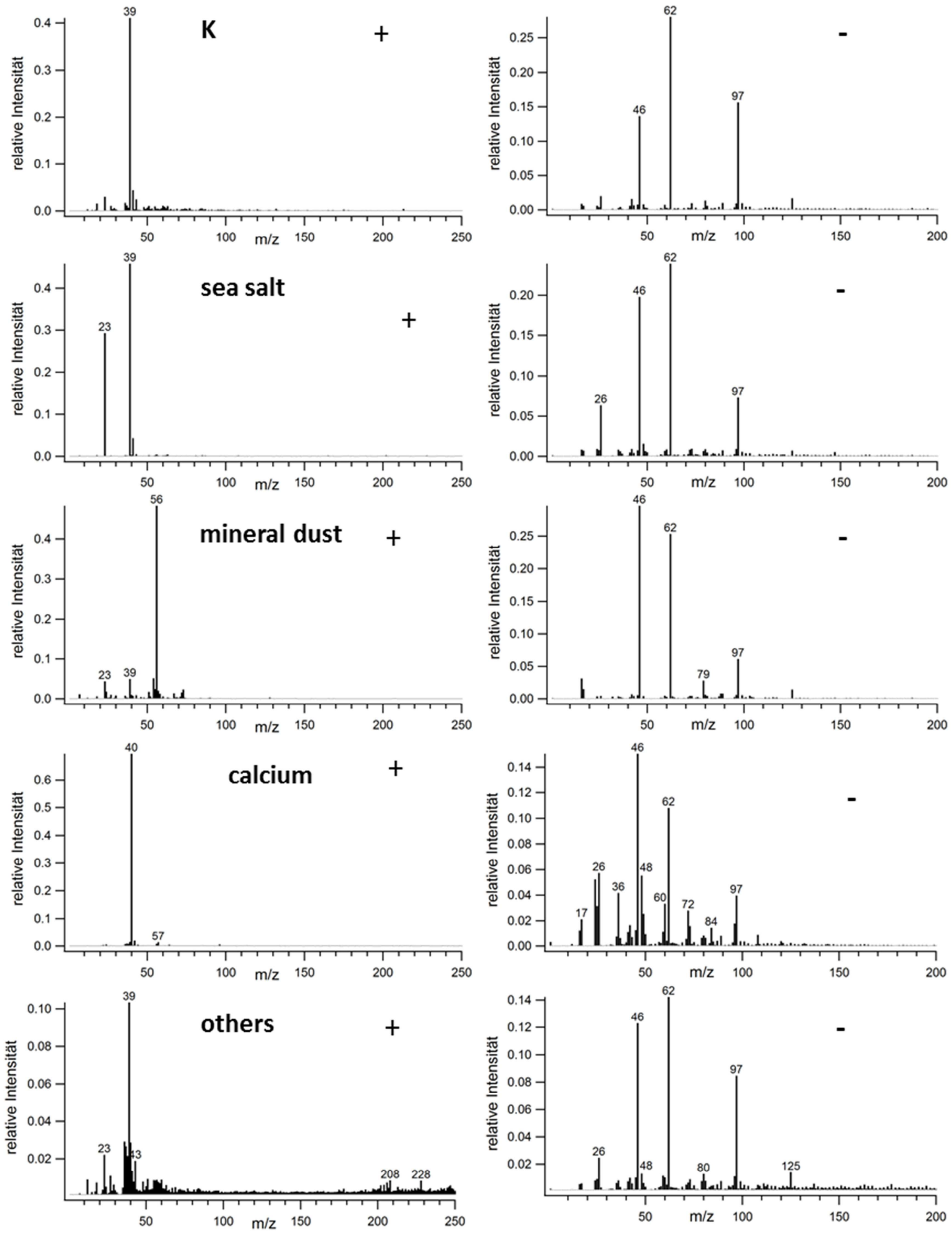

Figure S5: Mean positive (left) and negative (right) mass spectra representative of the particle types “K” (4 clusters), “sea salt”, “mineral dust”, “calcium” and “others”.

Table S1: Pearson correlation coefficients of the 19 representative mean cluster spectra plus “others”. Correlation coefficients greater than or equal to 0.7 are highlighted gray.

Particle type	org, K_1	org, K_2	org, K_3	org, K_4	org ,K_5	org	amines	soot_1	soot_2	diesel exhaust	soot, org 1	soot, org 2	biomass b._1	biomass b._2	biomass b._3	K	sea salt	min. dust	Ca	others
org, K_1	1	0.64	0.96	0.40	0.43	0.15	0.46	0.22	0.28	0.42	0.44	0.36	0.89	0.84	0.80	0.77	0.67	0.23	0.14	0,62
org, K_2		1	0.60	0.50	0.71	0.25	0.72	0.45	0.45	0.21	0.36	0.36	0.57	0.58	0.44	0.79	0.66	0.57	0.24	0,89
org,K_3			1	0.42	0.45	0.17	0.47	0.22	0.26	0.33	0.38	0.35	0.89	0.76	0.81	0.79	0.68	0.24	0.12	0,62
org,K_4				1	0.70	0.75	0.82	0.44	0.38	0.16	0.44	0.68	0.46	0.41	0.34	0.71	0.51	0.33	0.13	0,75
org,K_5					1	0.66	0.96	0.75	0.70	0.24	0.45	0.54	0.51	0.44	0.38	0.81	0.60	0.46	0.17	0,86
org						1	0.61	0.81	0.69	0.28	0.57	0.79	0.21	0.26	0.11	0.41	0.25	0.20	0.09	0,54
amines							1	0.58	0.53	0.18	0.40	0.52	0.53	0.45	0.40	0.85	0.62	0.46	0.17	0,88
soot_1								1	0.95	0.44	0.66	0.70	0.24	0.35	0.10	0.42	0.29	0.31	0.14	0,58
soot_2									1	0.63	0.79	0.70	0.30	0.47	0.11	0.41	0.30	0.31	0.17	0,56
diesel exhaust										1	0.88	0.62	0.36	0.73	0.20	0.20	0.25	0.11	0.30	0,30
soot, org_1											1	0.86	0.38	0.72	0.23	0.35	0.30	0.22	0.22	0,50
soot, org_2												1	0.33	0.57	0.23	0.42	0.32	0.24	0.21	0,59
biomass b._1													1	0.72	0.89	0.87	0.75	0.23	0.11	0,65
biomass b._2														1	0.61	0.63	0.71	0.26	0.18	0,61
biomass b._3															1	0.75	0.67	0.14	0.08	0,52
K																1	0.82	0.43	0.16	0,89
sea salt																	1	0.39	0.15	0,75
min. dust																		1	0.18	0,57
Ca																			1	0,34
others																				1

3. Marker peak classification

The software CRISP allows for the selection of mass spectra where the relative peak intensity (RI) of a given m/z value is above respectively below a threshold value. It is user-dependent which peak intensity is required for being counted as signal. Especially in case of low signals the determination of a threshold may be arbitrary and subjective. Therefore two different threshold values were chosen. A peak was defined **not** to be present in a mass spectrum if RI < 0.01, and to be present if RI > 0.03. These threshold values were determined empirically. This implies, however, that mass spectra where the selected marker peak intensity lies between these thresholds are not considered. Figure S6 presents the analysis of all single particle mass spectra during HCCT-2010 by marker peaks with respect to iron (Figure S6a, $RI_{m/z\ 56} > 0.03$). About 2038 mass spectra (1.1 %) fulfilled this criterion. Besides Fe^+ also Na^+ (m/z 23), C_3^+ (m/z 36), K^+ (m/z 39) and V^+ (m/z 51) are present in the average positive mass spectrum indicating the signature of mineral dust (Silva et al., 2000; Hinz et al., 2006; Dall'Osto et al., 2010). Vanadium originates rather from fuel combustion (Tolocka et al., 2004; Korn et al., 2007; Ault et al., 2010) and industrial sources like refineries (Dall'Osto et al., 2004; Ault et al., 2009) than mineral dust. Therefore the criterion was modified such that m/z 51 and m/z 67 (VO^+) should not appear in the mass spectra indicating iron. The mean mass spectrum of the selected particle spectra according to the criteria showed then only mineral dust (Na^+, K^+, Fe^+, Figure S6b). For further differentiation the criterion was changed, so that iron containing mass spectra should not indicate potassium (Figure S6c, $RI_{m/z\ 56} > 0.03$, $RI_{m/z\ 39} < 0.01$). As a result, the mean spectrum shows iron particles that are internally mixed with vanadium (m/z 51). Also spectra being dominated by vanadium (Figure S6d, $RI_{m/z\ 51} > 0.03$, $RI_{m/z\ 67} > 0.03$) reveal an internal mixture with iron. In this way two different iron containing particle types (mineral dust and iron internally mixed with vanadium) were identified and distinguished by their sources with this method. After the clustering, the fraction "others" was investigated additionally by marker peaks of lead ($RI_{m/z\ 208} > 0.03$), nickel ($RI_{m/z\ 58} > 0.03$), vanadium ($RI_{m/z\ 51}$, $RI_{m/z\ 67} > 0.03$) and iron ($RI_{m/z\ 56} > 0.03$). Furthermore, the mineral dust fraction resulting from the clustering and the iron fraction by the marker peak method were distinguished between mineral dust ($RI_{m/z\ 51}$, $RI_{m/z\ 67} < 0.01$) and iron internally mixed with vanadium ("Fe, V") belonging probably to an industrial source.

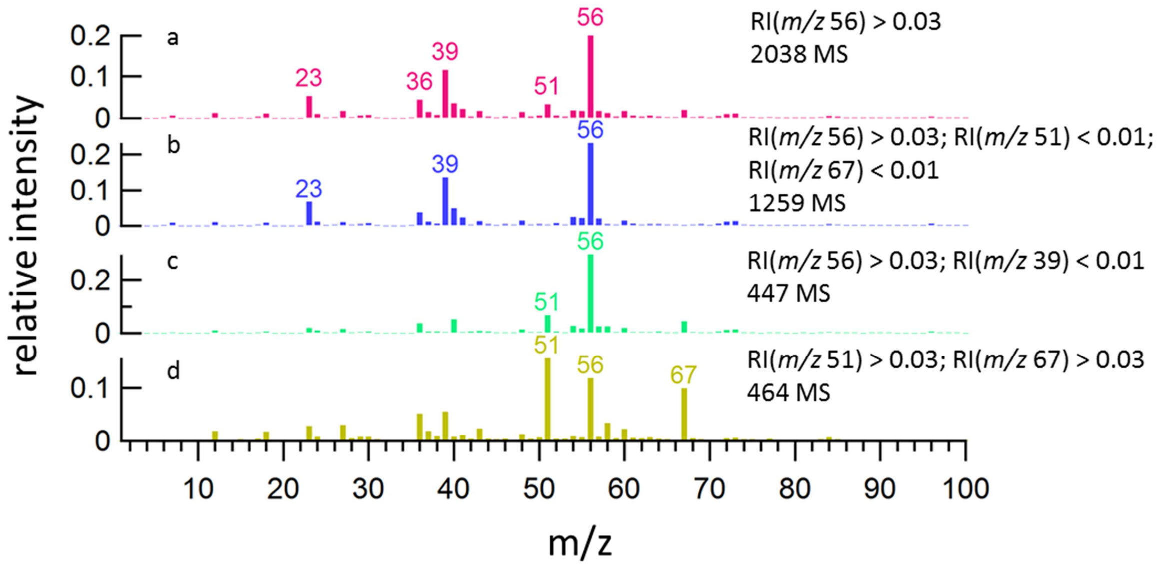

Figure S6: Mean positive mass spectrum of iron containing particles (a) being extracted from the HCCT-2010 data set by marker peaks. Mineral dust (b) and iron particles containing vanadium (c, d) from fuel combustion or industrial sources can be distinguished by specification of the criterion. Beneath the criterion, the number of filtered mass spectra is given.

References

Ault, A. P., Moore, M. J., Furutani, H., and Prather, K. A.: Impact of Emissions from the Los Angeles Port Region on San Diego Air Quality during Regional Transport Events, Environ. Sci. Technol., 43, 3500-3506, 10.1021/es8018918, 2009.

Ault, A. P., Gaston, C. J., Wang, Y., Dominguez, G., Thiemens, M. H., and Prather, K. A.: Characterization of the Single Particle Mixing State of Individual Ship Plume Events Measured at the Port of Los Angeles, Environ. Sci. Technol., 44, 1954-1961, 10.1021/es902985h, 2010.

Dall'Osto, M., Beddows, D. C. S., Kinnersley, R. P., Harrison, R. M., Donovan, R. J., and Heal, M. R.: Characterization of individual airborne particles by using aerosol time-of-flight mass spectrometry at Mace Head, Ireland, J. Geophys. Res.-Atmos., 109, 10.1029/2004jd004747, 2004.

Dall'Osto, M., Harrison, R. M., Highwood, E. J., O'Dowd, C., Ceburnis, D., Querol, X., and Achterberg, E. P.: Variation of the mixing state of Saharan dust particles with atmospheric transport, Atmos. Environ., 44, 3135-3146, 10.1016/j.atmosenv.2010.05.030, 2010.

Hinz, K. P., Erdmann, N., Gruning, C., and Spengler, B.: Comparative parallel characterization of particle populations with two mass spectrometric systems LAMPAS 2 and SPASS, Int. J. Mass Spectrom., 258, 151-166, 10.1016/j.ijms.2006.09.008, 2006.

Korn, M. D. A., dos Santos, D. S. S., Welz, B., Vale, M. G. R., Teixeira, A. P., Lima, D. D., and Ferreira, S. L. C.: Atomic spectrometric methods for the determination of metals and metalloids in automotive fuels - A review, Talanta, 73, 1-11, 10.1016/j.talanta.2007.03.036, 2007.

Silva, P. J., Carlin, R. A., and Prather, K. A.: Single particle analysis of suspended soil dust from Southern California, Atmos. Environ., 34, 1811-1820, 10.1016/s1352-2310(99)00338-6, 2000.

Tolocka, M. P., Lake, D. A., Johnston, M. V., and Wexler, A. S.: Number concentrations of fine and ultrafine particles containing metals, Atmos. Environ., 38, 3263-3273, 10.1016/j.atmosenv.2004.03.010, 2004.